Power dependence of upconversion luminescence in lanthanide and transition-metal-ion systems

M. Pollnau,* D. R. Gamelin, S. R. Lüthi,† and H. U. Güdel
Department of Chemistry and Biochemistry, University of Bern, Freiestrasse 3, CH-3012 Bern, Switzerland

M. P. Hehlen
Gemfire Corporation, 2471 East Bayshore Road, Palo Alto, California 94303
(Received 21 June 1999)

We show theoretically with the simplest possible model that the intensity of an upconversion luminescence that is excited by the sequential absorption of n photons has a dependence on absorbed pump power P, which may range from the limit of P^n down to the limit of P^1 for the upper state and less than P^1 for the intermediate states. The two limits are identified as the cases of infinitely small and infinitely large upconversion rates, respectively. In the latter case, the dependence of luminescence intensities from intermediate excited states on pump power changes with the underlying upconversion and decay mechanisms. In certain situations, energy-transfer upconversion and excited-state absorption can be distinguished by the measured slopes. The competition between linear decay and upconversion in the individual excitation steps of sequential upconversion can be analyzed. The influence of nonuniform distributions of absorbed pump power or of a subset of ions participating in energy-transfer upconversion is investigated. These results are of importance for the interpretation of excitation mechanisms of luminescent and laser materials. We verify our theoretical results by experimental examples of multiphoton-excited luminescence in $Cs_3Lu_2Cl_9:Er^{3+}$, $Ba_2YCl_7:Er^{3+}$, $LiYF_4:Nd^{3+}$, and $Cs_2ZrCl_6:Re^{4+}$.

I. INTRODUCTION

Spectroscopic data such as absorption and emission spectra, luminescent transients, and the pump-power dependence of luminescence intensities are essential to the understanding of excitation mechanisms in luminescent and laser materials and to the improvement of device performance. Special attention has been devoted to the investigation of upconversion-induced luminescence,[1,2] partly because of the availability of near-infrared pump sources for the excitation of visible luminescence[3–14] and laser emission[15–25] and partly because these mechanisms can introduce a loss channel for devices emitting in the infrared region.[26–34] The two most common excitation processes that lead to emission from energy states higher than the terminating state of the first pump-absorption step are energy-transfer upconversion (ETU) and pump excited-state absorption (ESA).

For the interpretation of short-wavelength luminescence, it is often assumed that the order n of the upconversion process, i.e., the number n of pump photons required to excite the emitting state, is indicated by the slope of the luminescence intensity versus pump power in double-logarithmic representation. However, as a consequence of the conservation of energy, a nonlinear process that transfers energy from one quantum state to another cannot maintain its nonlinear nature up to infinite excitation energy. A well-known example of this phenomenon from quantum optics is frequency conversion by second-harmonic generation. This process naturally exhibits a quadratic dependence of the second-harmonic energy versus fundamental energy, which levels off to a linear behavior when the conversion efficiency approaches unity. Similarly, the dependence of an upconversion-luminescence intensity on pump power is also expected to decrease in slope with increasing excitation, and a ''saturation'' of the intensity of an upconversion luminescence for higher pump powers was already observed 30 years ago.[35]

In this paper we investigate the physical nature of the ''saturation'' process. We shall show that the experimentally observed decrease in the slope of an upconversion-luminescence intensity versus pump power with increasing power is determined by the competition between linear decay and upconversion processes for the depletion of the intermediate excited states. The intensity of an upconversion luminescence that is excited by the sequential absorption of n photons has a dependence on absorbed pump power P, which may range from P^n in the limit of infinitely small upconversion rates down to P^1 for the upper state and less than P^1 for the intermediate states in the limit of infinitely large upconversion rates. Whereas the upper limit is valid universally, the lower limit for the intermediate states depends on whether the excitation is achieved by ETU or ESA and whether the states decay predominantly by luminescence to the ground state or relaxation into the next lower-lying state. The presented results are obtained from the solution of simple rate equations, confirmed by the numerical investigation of more complex situations, and illustrated by experimental examples. These results allow for the interpretation of a measured intensity-versus-power dependence of multiphoton-excited luminescence with respect to the order of the process and its physical origin and strength.

In the following section, we shall state the model assumptions and demonstrate the fundamental effect that rules the dependence of upconversion and downconversion luminescence intensities on pump power. More generalized solutions for the slopes of the luminescence intensities versus pump power will be derived in Sec. III. It will be discussed in Sec. IV how different excitation and decay mechanisms or the competition between upconversion and decay for individual steps of sequential upconversion can be distinguished using the measured slopes. In Sec. V, the influence of inhomoge-

neous distributions of absorbed pump power will be investigated, and we shall show how a fractional participation of active ions in ETU will manifest itself. Experimental examples will be presented in Sec. VI.

II. VARIATION OF LUMINESCENCE INTENSITIES WITH PUMP POWER: A SIMPLE MODEL

Throughout this paper, the expression ''the slope of the luminescence'' is used as a shortcut for the more precise statement ''the slope of the luminescence intensity in double-logarithmic representation versus absorbed pump power for a known pump focus,'' i.e., versus absorbed pump intensity.

A. Basic assumptions

The excitation mechanisms in systems with several metastable electronic excited states are usually rather complex. Besides excitation by ground-state absorption (GSA), subsequent upconversion by ESA and/or ETU, and depletion by luminescence and multiphonon relaxation, additional processes may occur: Cross relaxation between excited states or an avalanche process, three-ion energy transfer, energy transfer to other impurity ions, as well as amplified spontaneous emission and laser oscillation. Those additional mechanisms influence the excitation to or the relaxation from an excited state in a nonlinear way. In addition, a radially nonuniform pump profile, a longitudinally nonuniform pump absorption, ground-state bleaching, the distribution of ions in the host lattice, or any temperature dependence of an excitation or relaxation process have an influence on the luminescence intensities. Those situations shall not be considered in this section (for the investigation of a radially nonuniform pump profile, a longitudinally nonuniform pump absorption, ground-state bleaching, or the distribution of ions in the host lattice, see Sec. V). We assume here the simplest possible model.

(1) The ground-state population density is constant.

(2) The system is pumped continuous-wave by GSA.

(3) Upconversion steps between subsequent excited states take place by either ETU or ESA.

(4) The excited states i have lifetimes τ_i and decay with rate constants $A_i=\tau_i^{-1}$ either to their next lower-lying state or directly to the ground state.

In practice, the two different cases of (4) often correspond to a high-phonon-energy material with a predominant multiphonon-induced decay to the next lower-lying state (denoted in this paper by a branching ratio $\beta_i=1$) and a low-phonon-energy host material with a predominant radiative decay to the ground state ($\beta_i=0$), respectively. However, it is not important whether the decay mechanism is radiative or nonradiative, and there exist also examples of luminescence from an upper to an intermediate state with a high branching ratio β_i (see, e.g., our example in Sec. VI D). The assumptions of $\beta_i=1$ or $\beta_i=0$ simplify the solutions of the rate equations and are made here to exemplify the two extreme limiting scenarios.

Since ground-state bleaching is assumed to be negligible, the ground-state population density is

$$N_0 \approx \text{const.} \tag{1}$$

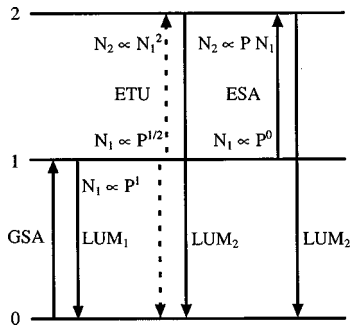

FIG. 1. Simple three-level upconversion scheme. Solid and dashed arrows indicate the radiative and nonradiative population and depopulation mechanisms for each level, respectively. The dependence of the population density N_1 on pump power for the corresponding depletion pathways, and the dependence of N_2 on N_1 are indicated for the different cases of ETU and ESA.

In the presence of ESA, the absorption coefficient α at the pump wavelength for a system with n excited levels is given by the sum of the absorption coefficients $\sigma_j N_j$ of the transitions from states j,

$$\alpha=\sum_{j=0,\ldots,n-1}\sigma_j N_j, \tag{2}$$

where σ_j is the absorption cross section from state j at the pump wavelength and N_j is its population density. For absorption over a sample length l, which is short compared to the absorption length α^{-1}, we expand the exponential function of the Lambert-Beer law for the calculation of absorbed pump power into a Taylor series and approximate it by the leading term:

$$1-\exp[-l\alpha]\approx l\alpha. \tag{3}$$

From Eqs. (2) and (3), it follows that the pump rate R_i of an individual transition from state i can be written as[36]

$$R_i=\frac{\lambda_p}{hcl\pi w_p^2}P\{1-\exp[-l\alpha]\}\frac{\sigma_i N_i}{\alpha}$$

$$\approx\frac{\lambda_p}{hc\pi w_p^2}P\sigma_i N_i=\rho_p\sigma_i N_i \tag{4}$$

with λ_p the pump wavelength, w_p the pump radius, P the incident pump power, h Planck's constant, and c the vacuum speed of light. The pump constant is

$$\rho_p=\frac{\lambda_p}{hc\pi w_p^2}P. \tag{5}$$

As a consequence of the assumption of small absorption, the pump rate at the transition from state i is independent of absorption at transitions from other states j in Eq. (4).

B. Competition of linear decay and upconversion

We first demonstrate the relevant effect that leads to a decrease in the slope of an upconversion luminescence with increasing pump power. The simplest system in which upconversion luminescence can be observed is a three-level system as depicted in Fig. 1. Assuming that the system is pumped by GSA and the upconversion step is achieved by

ETU with a corresponding parameter W_1, the rate equations describing the excitation mechanisms in this system are Eq. (1) and

$$dN_1/dt=\rho_p\sigma_0N_0-2W_1N_1^2-A_1N_1, \tag{6}$$

$$dN_2/dt=W_1N_1^2-A_2N_2. \tag{7}$$

Under steady-state excitation, this yields

$$A_2N_2=W_1N_1^2, \tag{8}$$

$$\rho_p\sigma_0N_0=2W_1N_1^2+A_1N_1. \tag{9}$$

It follows from Eq. (8) that

$$N_2\propto N_1^2. \tag{10}$$

If linear decay (LUM_1 in Fig. 1) is the dominant depletion mechanism of level 1, we can neglect the upconversion term in Eq. (9). It follows from Eqs. (5) and (9) that $N_1\propto P$ and, consequently, $N_2\propto N_1^2\propto P^2$, corresponding to one limit. In contrast, if upconversion (ETU in Fig. 1) is dominant, i.e., we can neglect the linear decay term in Eq. (9), then $N_1^2\propto P$ or $N_1\propto P^{1/2}$, resulting in $N_2\propto N_1^2\propto P$, corresponding to the other limit.

For intermediate pump powers, situations of competition between linear decay and depletion by upconversion are established and, consequently, the slopes of the luminescences are between the two limiting cases. For all pump powers, the slope of the upconversion luminescence is twice that of the downconversion luminescence because of Eq. (10).

We also solve here the simplest case involving ESA as the upconversion mechanism, i.e., the ETU process is replaced by the ESA process in Fig. 1. The rate equations, in this case, are Eq. (1) and

$$dN_1/dt=\rho_p\sigma_0N_0-\rho_p\sigma_1N_1-A_1N_1, \tag{11}$$

$$dN_2/dt=\rho_p\sigma_1N_1-A_2N_2. \tag{12}$$

From Eqs. (5) and (12), we find that $N_2\propto PN_1$. If the linear decay from level 1 is dominant and, thus, the ESA term is negligible in Eq. (11), we obtain $N_1\propto P$ and, consequently, $N_2\propto P\ N_1\propto P^2$. For strong ESA, the linear decay term can be neglected in Eq. (11), and we derive that N_1 is independent of P, resulting in $N_2\propto P\ N_1\propto P$.

This shows that, with increasing pump power and the resulting increasing importance of upconversion, the slope of the upconversion luminescence changes from quadratic to linear, whereas the slope of the directly excited luminescence changes from linear to less than linear, with different limits obtained for ETU and ESA. This behavior, therefore, fundamentally derives from the competitive mechanisms of upconversion and downconversion for the depletion of the intermediate excited state.

III. POWER DEPENDENCE: GENERALIZED SOLUTIONS

We now assume the energy-level scheme displayed in Fig. 2 having $n=4$ excited states. Under the basic assumptions made in Sec. II, we investigate the slopes of the upconversion luminescences for the following eight situations.

The upconversion mechanism is either (A) ETU or (B) ESA. We solve the rate equations for the cases of (1) small upconversion rates and short intrinsic lifetimes, i.e., luminescence dominates over upconversion as a depletion mechanism of the intermediate excited states, and (2) large upconversion rates and long intrinsic lifetimes, i.e., upconversion dominates depletion of the intermediate excited states. We investigate the influence of the following decay routes on the slopes of the luminescences: (i) Predominant decay to the next lower-lying state ($\beta_i=1$) or (ii) predominant luminescence directly to the ground state ($\beta_i=0$).

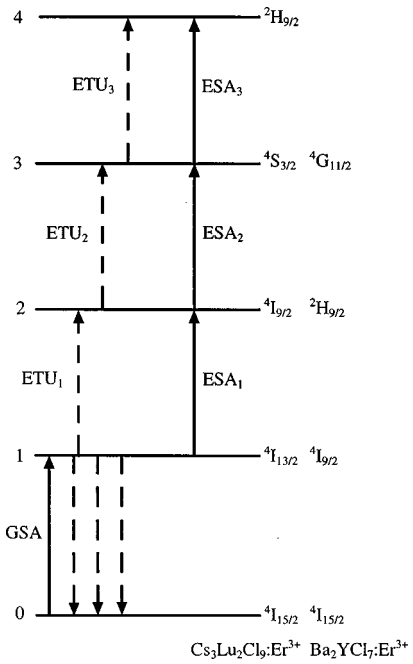

FIG. 2. Simple model for sequential four-step excitation. In our experimental examples of $Cs_3Lu_2Cl_9$:Er^{3+} excited at 1.54 μm and Ba_2YCl_7:Er^{3+} excited at 800 nm, these levels correspond to the electronic states indicated on the right-hand side. The radiative and nonradiative decay processes are not shown in the figure.

The generalized form of the dependence of upconversion-luminescence intensities on pump power is derived from the analytical solution of the rate equations for these more complex situations. For an overview, the results of this section are summarized in Table I.

A. Energy-transfer upconversion

If upconversion is achieved solely by ETU with corresponding parameters W_t, the rate equations for the excited-state population densities N_i are then given by Eq. (1) and

$$dN_1/dt=\rho_p\sigma_0N_0-2W_1N_1N_1-W_2N_1N_2-W_3N_1N_3-A_1N_1+\beta_2A_2N_2, \tag{13}$$

$$dN_2/dt=W_1N_1N_1-W_2N_1N_2-A_2N_2+\beta_3A_3N_3, \tag{14}$$

$$dN_3dt=W_2N_1N_2-W_3N_1N_3-A_3N_3+\beta_4A_4N_4, \tag{15}$$

$$dN_4/dt=W_3N_1N_3-A_4N_4. \tag{16}$$

TABLE I. Characteristic slopes of the steady-state excited-state population densities N_i of levels $i=1,\ldots,n$ and luminescences from these states for n-photon excitation. The investigated limits are: (1) small upconversion or (2) large upconversion by (A) ETU or (B) ESA, decay predominantly (i) into the next lower-lying state or (ii) by luminescence to the ground state, and (a) a small or (b) a large fraction of pump power absorbed in the crystal.

Influence of upconversion	Upconversion mechanism	Predominant decay route	Fraction of absorbed pump power	Power dependence	From level
(1) Small	ETU or ESA	next lower state or ground state	small or large	$N_i \sim P^i$	$i=1,\ldots,n$
(2) Large	(A) ETU	(i) next lower state	small or large	$N_i \sim P^{i/n}$	$i=1,\ldots,n$
		(ii) ground state	small or large	$N_i \sim P^{1/2}$	$i=1,\ldots,n-1$
				$N_i \sim P^1$	$i=n$
	(B) ESA	(i) next lower state	(a) small	$N_i \sim P^i$	$i=1,\ldots,n$
			(b) large	$N_i \sim P^{i/n}$	$i=1,\ldots,n$
		(ii) ground state	small or large	$N_i \sim P^0$	$i=1,\ldots,n-1$
				$N_i \sim P^1$	$i=n$

1. Small upconversion

For both, (i) $\beta_i=1$ and (ii) $\beta_i=0$, we obtain steady-state solutions of the type

$$N_i = A_1^{-i} \prod_{j=2,\ldots,i} [W_{j-1}A_j^{-1}](\rho_p\sigma_0 N_0)^i, \quad i=1,\ldots,n. \tag{17}$$

2. Large upconversion

The rate equations, for (i) $\beta_i=1$, have steady-state solutions for the population densities of the type

$$N_i = \prod_{j=2,\ldots,i} [W_{j-1}A_j^{-1}] \prod_{k=2,\ldots,n-1} [A_k^{i/n}] \times \prod_{l=1,\ldots,n-1} [W_l^{-i/n}](\rho_p\sigma_0 N_0)^{i/n}, \quad i=1,\ldots,n. \tag{18}$$

For (i) $\beta_i=0$, we obtain the following solutions:

$$N_i = 0.5 W_1^{0.5} W_i^{-1} (\rho_p\sigma_0 N_0)^{0.5}, \quad i=1,\ldots,n-1 \tag{19}$$

$$N_n = 0.25 A_n^{-1}\rho_p\sigma_0 N_0. \tag{20}$$

B. Excited-state absorption

If ESA is the relevant upconversion mechanism, the assumption that ground-state bleaching is negligible but upconversion luminescence is measurable implies that

$$\sigma_0 \ll \sigma_i,$$

$$\rho_p\sigma_0 \ll A_i \quad \text{for } i=1,\ldots,n. \tag{21}$$

The rate equations are then given by Eq. (1) and

$$dN_1/dt = \rho_p\sigma_0 N_0 - \rho_p\sigma_1 N_1 - A_1 N_1 + \beta_2 A_2 N_2, \tag{22}$$

$$dN_2/dt = \rho_p\sigma_1 N_1 - \rho_p\sigma_2 N_2 - A_2 N_2 + \beta_3 A_3 N_3, \tag{23}$$

$$dN_3/dt = \rho_p\sigma_2 N_2 - \rho_p\sigma_3 N_3 - A_3 N_3 + \beta_4 A_4 N_4, \tag{24}$$

$$dN_4/dt = \rho_p\sigma_3 N_3 - A_4 N_4. \tag{25}$$

1. Small upconversion

For both (i) $\beta_i=1$ and (ii) $\beta_i=0$, we obtain steady-state solutions of the type

$$N_i = \prod_{j=1,\ldots,i} [A_j^{-1}]\rho_p^i \prod_{j=1,\ldots,i} [\sigma_{j-1}]N_0, \quad i=1,\ldots,n. \tag{26}$$

2. Large upconversion

For $\beta_i=1$, the solution Eq. (26) is obtained. For (ii) $\beta_i=0$, the solutions for the population densities read

$$N_i = (\sigma_0/\sigma_i)N_0, \quad i=1,\ldots,n-1, \tag{27}$$

$$N_n = A_n^{-1}\rho_p\sigma_0 N_0. \tag{28}$$

In Eq. (26) and Eqs. (27) and (28), all excited-state population densities are small compared to N_0 because of Eq. (21).

The eight situations investigated above result in four different characteristic slopes for the excited-state population densities and luminescences from these states as indicated in Table I. To obtain these results, we inserted Eq. (5) in Eqs. (17)–(20) and (26)–(28). Note that other scenarios involving, e.g., cross relaxation between excited states, an avalanche process, three-ion energy transfer, or ground-state bleaching have been neglected for simplicity, but are expected to lead to significant deviations from the results of this model in certain experimental circumstances.

IV. POWER DEPENDENCE: SPECIFIC SITUATIONS

A. The limiting cases of small and large upconversion

With the results of Table I, the measurement of the slopes of multiphoton-excited luminescences enables an interpretation of the underlying upconversion mechanism and its strength. Generally, a measured slope of x is indicative of an upconversion process, which involves at least n photons, where n is the smallest integer greater than x (or equal to x if x is an integer). However, it may also be a higher-order process.

Low absorbed pump intensities and the consequent dominance of linear decay for the depletion of the intermediate excited states [case I of Table I] allow for the determination

of the order i of each excitation process, i.e., the number i of pump photons required to excite the emitting state. At high absorbed pump intensities, upconversion becomes the main depletion process of the intermediate excited states, allowing for the determination of the upconversion mechanism involved. If luminescence to the ground state overpowers relaxation to the next lower-lying state, the mechanisms of ETU [case (2)(A)(ii)] and ESA [case (2)(B)(ii)] can be distinguished by the slopes of the luminescences from intermediate excited states, which are $P^{1/2}$ in the case of ETU and P^0 in the case of ESA. If decay occurs mainly into the next lower-lying state and the fraction of pump power absorbed in the sample is small, ETU manifests itself in slopes of $P^{i/n}$ [case (2)(A)(i)], where ESA leads to slopes of P^i [case (2)(B)(i)(a)].

If the orders of the processes are known, the measured slopes indicate whether linear decay [case (1)] or upconversion [case (2)] dominates for a given absorbed pump intensity, with only one exception [case (2)(B)(i)(a) exhibits the same slope as case (1)].

B. Competitiveness of individual upconversion steps in sequential upconversion excitation

Experimentally, lifetimes and ETU or ESA rates are usually different for different excited states. As a consequence, some upconversion steps may be efficient compared to luminescence from their initial states for a given pump power, whereas other upconversion steps may be inefficient, especially when competing with fast multiphonon-relaxation processes. This possibility shall be investigated analytically for the example of Fig. 2.

We solve the rate equations (1) and (13)–(16) corresponding to the system of Fig. 2 for the case of ETU as the upconversion mechanism and luminescence to the ground state ($\beta_i = 0$) as the linear-decay mechanism, but with the following modifications: We assume that the first upconversion step ETU_1 is more efficient than downconversion luminescence whereas the upconversion steps ETU_2 and ETU_3 are inefficient. When neglecting the rate terms in Eqs. (13)–(16) that correspond to inefficient processes for the depletion of the corresponding states, we find that the steady-state solutions for the excitation densities exhibit slopes of $N_i \propto P^{i/2}$. The first and second excited states show slopes of $P^{1/2}$ and P^1, respectively, which would be expected from the system of Fig. 1 at high pump power, for the case of ETU as the upconversion mechanism. Levels 3 and 4 are not relevant for the dynamics of levels 1 and 2, because ETU_2 and ETU_3 are inefficient.

On the other hand, if only the second upconversion step ETU_2 were more efficient than downconversion luminescence from the corresponding initial state, whereas ETU_1 and ETU_3 were inefficient, we would find slopes of P^1 for luminescence from the first excited state and P^{i-1} for luminescence from the higher-lying states i. The two examples are, thus, distinguishable by the slopes of the observed luminescences. In this way, the competitiveness of individual upconversion steps in a multistep process can be determined from the measured slopes of upconversion luminescences.

V. COMMON DEVIATIONS FROM THE BASIC ASSUMPTIONS

A. Large pump absorption

If the sample length l is not small compared to the absorption length α^{-1}, a nonuniform longitudinal distribution of the absorbed pump power over the sample length obtains. This results in a longitudinal variation of the GSA pump rate and excitation density and, consequently, of the importance of upconversion along the pump-beam path through the sample.

If a large fraction of the pump power is absorbed in the sample, e.g., by choosing a longer sample, the left-hand side of Eq. (3) approaches unity and Eq. (4) becomes

$$R_i \approx \frac{\rho_p}{l} \frac{\sigma_i N_i}{\sum_{j=0,\ldots,n-1} \sigma_j N_j}. \tag{29}$$

In this case, the pump rate at the transition from state i depends on the absorption of pump power due to transitions from other states j, and solving the rate equations becomes more complex. In addition, integration over the sample length is no longer acceptable, because the different longitudinal parts exhibit different excited-state population densities and contribute in different ways to the luminescence intensities and must be treated individually. It is, therefore, more convenient to solve the rate equations numerically, with longitudinal resolution and under consideration of pump absorption according to a Lambert-Beer law. The corresponding computer code is described in Refs. 33 and 34.

For the case of small absorption, the limits of the slopes of the eight different situations described in Sec. III are confirmed by numerical examples. If the sample length and, thus, the fraction of pump power absorbed in the sample are increased in the calculation, the slopes of the excited-state population densities and luminescences from these states remain the same in seven of the eight investigated cases. In the case of large ESA rates, long excited-state lifetimes, and predominant decay to the next lower-lying state [case (2)(B)(i) of Table I], however, we find a different result: With the change from (a) small absorption (sample length l small compared to the absorption length α^{-1}) to (b) large absorption ($l > \alpha^1$), the slope of the population density of state i and luminescence from this state decreases continuously from $N_i \propto P^i$ to $P^{i/n}$. The reason is the direct dependence of the individual pump rates of Eq. (29) on each other.

The surprising fact that only one of the eight cases exhibits a dependence on crystal length can be understood in the following way. The difference between Eqs. (4) and (29) is only relevant if the upconversion mechanism is ESA and if the influence of ESA is large. It follows that the slopes do not change with increasing crystal length in those cases involving ETU or small ESA. In the case of large ESA [case (2)(B) of Table I], the response of the system to an increasing crystal length is a decreasing slope of the upconversion luminescences. If all states decay predominantly by luminescence to the ground state [case (2)(B)(ii) of Table I], however, the resulting slopes are already the smallest possible that can be expected. This leaves only one case [case (2)(B)(i) of Table I] sensitive to the direct dependence of the individual pump rates on each other.

The influence of ground-state bleaching is often an impor-

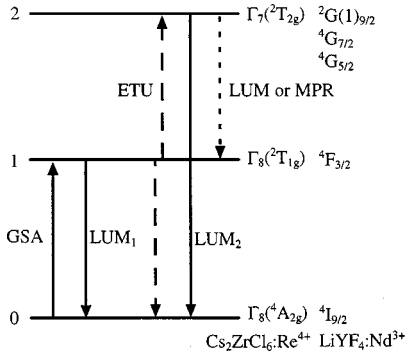

FIG. 3. Three-level upconversion scheme for the case of ETU as the upconversion mechanism. Solid and dashed arrows indicate the radiative and nonradiative population and depopulation mechanisms for each level, respectively. In our experimental examples of $Cs_2ZrCl_6:Re^{4+}$ excited at 1.047 μm and $LiYF_4:Nd^{3+}$ excited at 800 nm, these levels correspond to the electronic states indicated on the right-hand side. The dotted arrow from level 2 to level 1 indicates a luminescence (LUM) in the case of $Cs_2ZrCl_6:Re^{4+}$ and a multiphonon relaxation (MPR) in the case of $LiYF_4:Nd^{3+}$.

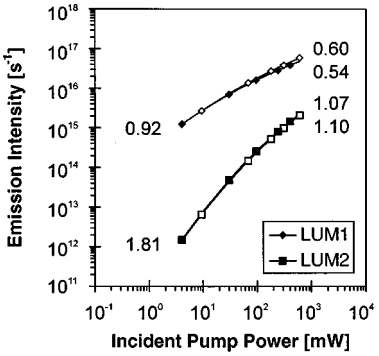

FIG. 4. Comparison of the calculated slopes of downconversion (LUM_1) and upconversion (LUM_2) luminescences in the level scheme of Fig. 3, assuming a flat-top (solid symbols) or a Gaussian (open symbols) radial pump profile. The numbers denote the slope in double-logarithmic representation at low and high pump power, respectively.

tant issue, because it may strongly affect device performance. Nevertheless, it will not be discussed in this paper because of the following reasons. First, ground-state bleaching depends on many parameters and cannot easily be described without taking the complete rate-equation system into account. Second, if there is no lifetime quenching by cross relaxation, which would depend on the ground-state population density, the influence of ground-state bleaching on the slopes of upconversion luminescences can be eliminated, in the case of ETU as the upconversion mechanism, by plotting the luminescence intensities versus absorbed instead of incident pump power. If ESA is the dominating upconversion mechanism, however, this simple method is not applicable. In this case, situations may occur where an increasing pump power leads to ground-state bleaching and a consequent decrease in GSA rate combined with an increase in ESA rate, resulting in depletion of the intermediate excited state and a decrease in luminescence intensity from this level; cf. Fig. 8(b) of Ref. 37. In this case, ground-state bleaching has to be considered in the rate equations.

B. Gaussian pump profile

A nonuniform transverse distribution of the pump power over the sample cross section arises, for example, from a Gaussian pump profile. This results in a radial variation of the excitation density and, consequently, of the importance of upconversion across the transverse profile of the beam. We investigate here numerically the influence of a Gaussian pump profile on the three-level system shown in Fig. 3. The parameters and rate equations used for the calculation are taken from Ref. 38. They correspond to the experimental example of $LiYF_4$:1% Nd^{3+} (Sec. VI C).

The result of the calculation is shown in Fig. 4. The slope of the downconversion luminescence (LUM_1) decreases slightly slower from P^1 toward $P^{0.5}$ with increasing pump power for a Gaussian pump profile (open symbols) compared to a flat-top pump profile (solid symbols), because the ions in the wings of the Gaussian profile exhibit less ETU. The slopes of the upconversion luminescence (LUM_2), which decrease from P^2 toward P^1 exhibit even less deviation between a Gaussian and a flat-top pump profile. A similar situation obtains when the ETU process is replaced by an ESA process (cf. Fig. 1) in the calculation. Generally, the differences in the slopes when using a Gaussian or a flat-top pump profile are small.

In contrast, a much larger influence of the Gaussian pump profile on the slope of the upconversion luminescence is found in the case of an avalanche process.[39] The reason for this behavior is the strong dependence of the absorption coefficient on pump power, which introduces a highly nonlinear response of the system over the Gaussian pump profile in the case of an avalanche process.

C. Participation of a subset of ions in energy-transfer upconversion

ETU is an interionic process whose probability depends strongly on the distance between the participating ions.[40] ETU is, therefore, influenced by the host geometry, the dopant concentration, energy migration between the active ions, and the statistical (or nonstatistical) distribution of active ions in a host material. Commonly, the active impurity ions are randomly distributed in the host lattice. Some of them have a closer nearest neighbor than others and, thus, exhibit a higher probability of being involved in an ETU process.[41] In some cases, a fraction of ions may be isolated, arranged in clusters,[42] or occupy different sites in the host lattice for the active ions with different nearest-neighbor distances.[43]

It is the purpose of this section to demonstrate the fundamental influence of the presence of different ion classes in the host lattice on the slopes of the luminescences. In the following, we choose again the simplest possible model. We assume that there exist two different ion classes: one class of ions that are involved in ETU and one class of ions that do not contribute to ETU.

In the absence of ESA, the measurement of the slopes of upconversion and downconversion luminescences provides a simple method to probe the fraction of ions that participates in ETU. For this class of ions, the coupling of the rate equations (6) and (7), resulting in Eq. (10), requires that a decrease of the slope of the upconversion luminescence from a quadratic to a linear behavior is accompanied by a corresponding decrease of the slope of the downconversion lumi-

nescence from a linear to a square-root behavior. In contrast, isolated ions will not contribute to upconversion luminescence and show a linear slope of their downconversion luminescence throughout the whole pump-power range. The observed downconversion-luminescence intensity is the sum of the contributions from each class of ions.

Since a linear function increases faster than a square-root function, the intensity of downconversion luminescence from those ions that do not participate in ETU will eventually overpower the corresponding luminescence intensity from ions exhibiting upconversion losses. It follows that the slope of the downconversion luminescence will first decrease with increasing pump power and, consequently, increasing upconversion losses. With further increasing pump power, the luminescence intensity of isolated ions will contribute an increasingly significant fraction to the overall intensity of downconversion luminescence. The slope of the downconversion luminescence will, therefore, increase again.

This behavior is calculated for the simple situation of Fig. 3, assuming a constant dopant concentration, but different fractions of ions participating in ETU. (An experimental example is presented later in Sec. VI D along with calculated curves; cf. Fig. 8.) If 100% of the ions participate in ETU, the results of Sec. II are derived: The slopes of downconversion (L_1) and upconversion (L_2) luminescences decrease from P^1 to $P^{0.5}$ and from P^2 to P^1, respectively. If a significant fraction of ions does not participate in ETU, the slope of the downconversion luminescence first decreases from P^1 but then returns to P^1 at higher pump powers, with the turning point moving to a smaller pump power for an increasing fraction of isolated ions.

The influence of a Gaussian pump profile (or, generally, a macroscopically inhomogeneous excitation density) on the slope of the downconversion luminescence is different from the influence of several ion classes that may or may not participate in ETU. A Gaussian pump profile results in a variation of the excitation density N_1 in the intermediate state for a given pump power, whereas the effect described here arises from a difference in the ETU parameter W_1 for different ion classes. The influence of the Gaussian pump profile on the slope of the downconversion luminescence is small, because those regions in the wings of the pump profile with a smaller excitation density N_1 naturally contribute less to the luminescence intensity. On the other hand, several ion classes may have a large influence on the slope, because all these ion classes may be present in the center of the Gaussian pump profile.

VI. EXPERIMENTAL EXAMPLES

Four experimental examples shall illustrate the theoretical results of Secs. II–V. For detailed discussions of the excitation mechanisms in the four systems chosen here, see Refs. 38 and 44–48.

A. Four-step upconversion in $Cs_3Lu_2Cl_9$:Er^{3+}

The similar energy gaps of four excitation steps in Er^{3+} and the low phonon energies in a chloride make the $Cs_3Lu_2Cl_9$:Er^{3+} system a prominent example of efficient four-step upconversion with subsequent intense luminescence from all states along the excitation pathway. This system shall serve as an example for two of the results of Table I. We have investigated two-, three-, and four-photon excitation in samples of $Cs_3Lu_2Cl_9$:1% Er^{3+} and $Cs_3Er_2Cl_9$.[44] The Er^{3+} ions were excited at 1.54 μm along the excitation pathway $^4I_{15/2}\rightarrow{}^4I_{13/2}\rightarrow{}^4I_{9/2}\rightarrow{}^4S_{3/2}\rightarrow{}^2H_{9/2}$. These levels correspond to levels 0–4 in Fig. 2, with other intermediate excited states of erbium not shown in this figure. The slopes of the ground-state luminescences from the $^4I_{9/2}$ (two-photon upconversion), $^4S_{3/2}$ (three-photon upconversion), and $^2H_{9/2}$ levels (four-photon upconversion) at 800 nm, 550 nm, and 420 nm, respectively, was measured (Fig. 5). Because of the low phonon energies the excited states exhibit only small multiphonon-relaxation rates and decay predominantly by luminescence to the ground state. In the 1%-doped sample, the upconversion steps are achieved partly by ESA and partly by ETU, whereas for the 100%-doped sample, the dominant upconversion mechanism is ETU.[44]

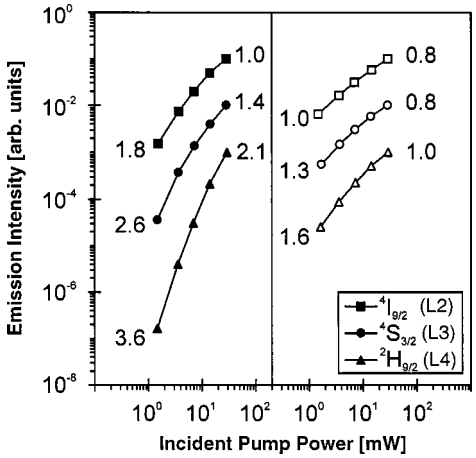

FIG. 5. Measured emission intensities from the $^4I_{9/2}$ (two-photon excitation), $^4S_{3/2}$ (three-photon excitation), and $^2H_{9/2}$ (four-photon excitation) levels at 800 nm, 550 nm, and 420 nm, respectively, in $Cs_3Lu_2Cl_9$:1% Er^{3+} (solid symbols) and $Cs_3Er_2Cl_9$ (open symbols) vs pump power, after excitation at 1.54 μm into $^4I_{3/2}$ (Ref. 44). The numbers denote the slope in double-logarithmic representation at low and high pump power, respectively.

We compare here the two extreme experimental situations of either predominant linear decay or strong upconversion with the corresponding limiting cases of Table I. At low pump powers in the 1%-doped sample where upconversion mechanisms have a small influence (Fig. 5, left-hand side), the slopes approach the limit of P^i for an i-photon-excited luminescence [case (1) of Table I]. On the other hand, at high pump powers in the 100%-doped sample where ETU is the dominant excitation and depletion mechanism (Fig. 5, right-hand side), the slopes approach the limit of $P^{1/2}$ for luminescences from the intermediate excited states and P^1 for luminescence from the upper excited state $^2H_{9/2}$ [case (2)(A)(ii) of Table I]. For increasing pump powers in the 1%-doped sample as well as for decreasing pump powers in the 100%-doped sample, situations of competition between linear decay and upconversion are found and the luminescences exhibit slopes that are between the two limiting cases.

B. Competitiveness of individual upconversion steps in Ba_2YCl_7:Er^{3+}

Another excitation sequence leading to population of $^2H_{9/2}$ in Er^{3+}-doped low-phonon host materials is a two-step

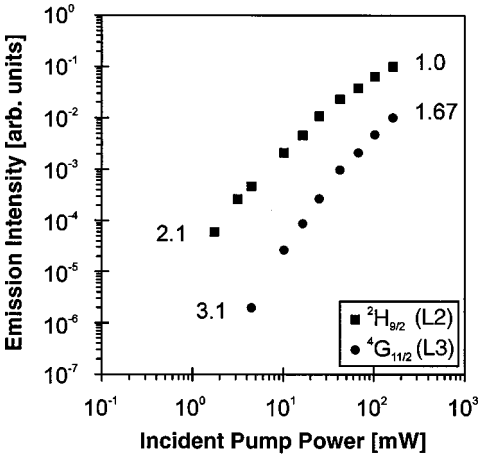

FIG. 6. Measured emission intensities from the $^2H_{9/2}$ (two-photon excitation) and $^4G_{11/2}$ (three-photon excitation) levels at 406.9 and 381.6 nm, respectively, in Ba_2YCl_7:3.2% Er^{3+} vs pump power, after excitation at 800 nm into $^4I_{9/2}$, respectively (Ref. 46). The numbers denote the slope in double-logarithmic representation at low and high pump power, respectively.

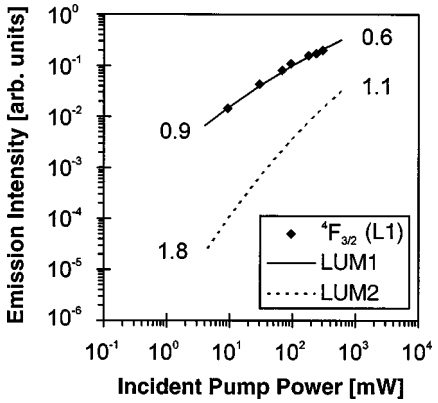

FIG. 7. Measured emission intensity (diamonds) of downconversion luminescence from the $^4F_{3/2}$ level (single-photon excitation) at 1.05 μm in $LiYF_4$:Nd^{3+} vs absorbed pump power, after excitation at 800 nm into $^4F_{5/2}$ (Ref. 38). Also shown are calculated curves of the downconversion (solid line) and upconversion (dotted line) luminescence intensities, assuming that 100% of the Nd^{3+} ions participate in ETU. The calculation considers a Gaussian radial pump profile. The numbers denote the calculated slopes in double-logarithmic representation at low and high pump power, respectively.

excitation $^4I_{15/2}\rightarrow{}^4I_{9/2}\rightarrow{}^2H_{9/2}$ around 800 nm. The upconversion step may take place by ESA or ETU, depending on host material, exact pump wavelength, and dopant concentration. Luminescence from $^4G_{11/2}$ occurs after a second upconversion step by ETU, which may originate in any state above $^4I_{9/2}$.[45] The $^4I_{9/2}$, $^2H_{9/2}$, and $^4G_{11/2}$ levels correspond to levels 1, 2, and 3 in Fig. 2, respectively, with other intermediate excited states of erbium not shown in this figure. In Ba_2YCl_7:3% Er^{3+}, we have investigated the slopes of the upconversion luminescences from $^2H_{9/2}$ at 407 nm and $^4G_{11/2}$ at 382 nm, after excitation at 800 nm into $^4I_{9/2}$.[46]

The measured slopes of the upconversion luminescences (Fig. 6) change from $P^{2.1}$ to $P^{1.0}$ for $^2H_{9/2}$ and from $P^{3.1}$ to $P^{1.67}$ for $^4G_{11/2}$, with increasing pump power. Comparison with the theoretical results presented in Sec. V B suggests that the first upconversion step to $^2H_{9/2}$ becomes competitive with luminescent decay already at the highest pump power applied in our experiment, whereas the second upconversion step to $^4G_{11/2}$ remains relatively inefficient at this pump power. The slopes of the upconversion luminescences predicted for this case are $P^{i/2}$ for i-step upconversion (Sec. V B), in reasonable agreement with the measured slopes of $P^{1.0}$ for two-step upconversion into $^2H_{9/2}$ and $P^{1.67}$ for three-step upconversion into $^4G_{11/2}$.

C. Complete energy-transfer upconversion in $LiYF_4$:Nd^{3+}

The slope of the downconversion luminescence has been measured in $LiYF_4$:1% Nd^{3+}.[38] The Nd^{3+} ions were excited at 800 nm into the $^4F_{5/2}$ level. Subsequent fast multiphonon relaxation leads to the population of the $^4F_{3/2}$ level, which is the upper laser level of the well-known 1-μm Nd^{3+} laser transition. ETU from $^4F_{3/2}$ populates the $^2G(1)_{9/2}$, $^4G_{7/2}$, and $^4G_{5/2}$ levels. These states decay by fast multiphonon relaxation back to the $^4F_{3/2}$ level and can, therefore, be treated as a single state for our purposes.[38] Thus, $^4F_{3/2}$ corresponds to level 1 and $^2G(1)_{9/2}$, $^4G_{7/2}$, and $^4G_{5/2}$ correspond to level 2 in Fig. 3. The other excited states of Nd^{3+} are not shown in this figure. Since at the time of the experiment we were mostly interested in the lifetime quenching of $^4F_{3/2}$ by ETU and less in the weak upconversion luminescence from upper states, only downconversion luminescence at 1.05 μm was measured in the experiment.

The slope of the downconversion luminescence from $^4F_{3/2}$ in $LiYF_4$:1% Nd^{3+} exhibits a decrease from $P^{0.9}$ to $P^{0.6}$ in the experimental range of pump powers (diamonds in Fig. 7). This roughly approximates a decrease of the slope from the limit of P^1 at low pump power to $P^{0.5}$ at high pump power. Also shown is a calculated curve of the downconversion-luminescence intensity (solid line),[38] assuming that 100% of the Nd^{3+} ions participate in ETU. According to the findings of Sec. V C, we conclude from these results that in $LiYF_4$:1% Nd^{3+} most of the ions are involved in ETU. Consequently, the slope of the corresponding upconversion luminescence must then decrease from P^2 to P^1 (the dotted line in Fig. 7 represents the corresponding calculated curve), because in this case the two slopes are correlated to each other according to Eq. (10).

D. Fractional energy-transfer upconversion in Cs_2ZrCl_6:Re^{4+}

The Cs_2ZrCl_6:Re^{4+} system[47,48] is a rare example of a transition-metal-ion system showing upconversion luminescence from a second metastable excited state. In Cs_2ZrCl_6:3.2% Re^{4+}, we have investigated the slopes of the luminescences from the $\Gamma_8(^2T_{1g})$ and $\Gamma_7(^2T_{2g})$ excited states. These excited states correspond to levels 1 and 2 in Fig. 3, respectively. The other excited states of Re^{4+} are not shown in this figure. After excitation of the system by GSA at the pump wavelength of 1047 nm, fast multiphonon relaxation populated the metastable $\Gamma_8(^2T_{1g})$ level. The upconversion step to $\Gamma_7(^2T_{2g})$ was achieved by ETU.[47,48]

The measured slope (Fig. 8) of the upconversion luminescence at 730 nm from $\Gamma_7(^2T_{2g})$ decreases with increasing pump power from P^2 to $P^{1.1}$ within our experimental power limits. These values are consistent with the theoretical limits

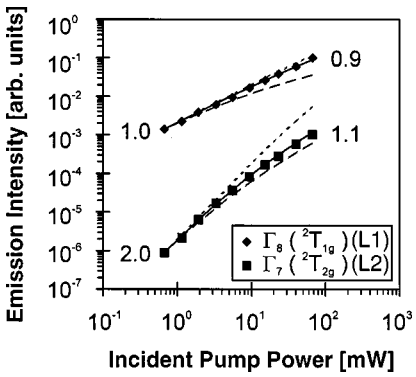

FIG. 8. Measured emission intensities from the $\Gamma_8(^2T_{1g})$ (single-photon excitation) and $\Gamma_7(^2T_{2g})$ (two-photon excitation) levels at 1.3 μm and 730 nm, respectively, in Cs_2ZrCl_6:3.2% Re^{4+} vs pump power, after excitation at 1.047 μm into $\Gamma_8(^2T_{1g})$ (Ref. 48). Also shown are calculated curves, assuming that 100% (dashed lines), 40% (solid lines), or 1% (dotted lines) of the Re^{4+} ions participate in ETU. The calculation assumes a Gaussian radial pump profile. The numbers denote the experimental slope in double-logarithmic representation at low and high pump power, respectively.

of P^2 at low pump power and P^1 at high power. The slope of the downconversion luminescence at 1.3 μm from $\Gamma_8(^2T_{1g})$, however, only changes from P^1 at low power to $P^{0.9}$ at high power. It is, thus, not correlated to the slope of the upconversion luminescence. This experimental finding is in clear contradiction to the result of Eq. (10), which predicts a correlation, i.e., a decrease in slope of the downconversion luminescence from P^1 to $P^{0.5}$ in the same power range as the corresponding upconversion luminescence decreases from P^2 to P^1.

At the simplest level, this observation can be interpreted as reflecting a scenario in which only a certain fraction of excited Re^{4+} ions participates in ETU. This fraction exhibits a slope of its downconversion luminescence, which decreases to a square-root behavior with increasing pump power. In the upconversion luminescence, we only probe this fraction of the excited ions, and observe a slope that decreases to a linear behavior with increasing pump power. The other fraction of excited Re^{4+} ions is excluded from ETU. It luminesces from level 1 to the ground state with a linear slope at all powers (see Sec. V C).

Based on this interpretation, we have calculated the slopes of the downconversion and upconversion luminescences with the spectroscopic parameters of Cs_2ZrCl_6:3.2% Re^{4+},[48] for different fractions of ions participating in ETU. Selected results are shown in Fig. 8. The model shows agreement with the measured slopes for a fraction of $40(\pm 10)\%$ of the ions participating in ETU. Although the theoretical method presented in Sec. V C is based on strong simplifications, it illustrates the important principle that upconversion and downconversion measurements need not probe the identical set of dopant ions, and this situation can be identified experimentally.

VII. CONCLUSIONS

Assuming the simplest possible n-photon upconversion excitation schemes, we have shown in a general way that the commonly assumed slope of the luminescence of P^n refers to the case of infinitely small upconversion rates. A realistic upconversion system that produces detectable upconversion luminescence will exhibit an intensity-versus-power dependence, which is less than P^n. Higher pump power and, consequently, increasing competition between linear decay and upconversion for the depletion of the intermediate excited states result in a significantly reduced slope. In most of the investigated cases, if upconversion dominates over linear decay for the depletion of the intermediate excited states, the slope of the luminescence from the upper state n is almost linear. The slopes of the luminescences from intermediate excited states are even less than linear and, in the case of ESA as the upconversion mechanism and ground-state luminescence as the decay mechanism, are almost independent of pump power.

The above results allow for the interpretation of the slope of a multiphoton-excited luminescence with respect to the order of the process and its physical origin and strength. In addition, the measurement of the slopes of upconversion and downconversion luminescences provides a method to investigate the fraction of ions that participate in ETU. With accurate measurements and a detailed model, it should be possible with this method to probe the influence of energy migration on ETU or spatial distributions of ions in crystalline lattices or glass matrices.

It has been the purpose of this paper to point out that fundamentally important information is contained in the measured dependence of upconversion-luminescence intensities on pump power. The population mechanisms found in real systems are often more complex than the basic models presented here. However, the fundamental equations presented in this paper can be adjusted or expanded to a specific situation.

ACKNOWLEDGMENTS

We thank Rozenn Burlot-Loison from our institute and Paul J. Hardman from the Optoelectronics Research Center, University of Southampton, United Kingdom for their contributions to the experiments, as well as Ralph Schenker and Markus Wermuth from our institute for helpful discussions. This work was partially supported by the Swiss National Science Foundation.

*Present address: Institute of Applied Optics, Department of Microtechnique, Swiss Federal Institute of Technology, CH-1015 Lausanne, Switzerland. FAX: ++41-31-631 43 99. Electronic address: pollnau@iac.unibe.ch

†Present Address: Department of Chemistry, The University of Queensland, Brisbane QLD 4072, Australia.

[1] F. Auzel, Proc. IEEE **61**, 758 (1973).

[2] J. C. Wright, Top. Appl. Phys. **15**, 239 (1976).

[3] M. Malinowski, B. Jacquier, M. Bouazaoui, M. F. Joubert, and C. Linares, Phys. Rev. B **41**, 31 (1990).

[4] N. J. Cockroft, G. D. Jones, and D. C. Nguyen, Phys. Rev. B **45**, 5187 (1992).

[5] A. Gharavi and G. L. McPherson, Chem. Phys. Lett. **200**, 279 (1992).
[6] A. T. Stanley, E. A. Harris, T. M. Searle, and J. M. Parker, J. Non-Cryst. Solids **161**, 235 (1993).
[7] M. Mujaji, G. D. Jones, and R. W. G. Syme, Phys. Rev. B **48**, 710 (1993).
[8] M. P. Hehlen, K. Krämer, H. U. Güdel, R. A. McFarlane, and R. N. Schwartz, Phys. Rev. B **49**, 12 475 (1994).
[9] M. P. Hehlen, G. Frei, and H. U. Güdel, Phys. Rev. B **50**, 16 264 (1994).
[10] T. Riedener, H. U. Güdel, G. C. Valley, and R. A. McFarlane, J. Lumin. **63**, 327 (1995).
[11] M. Wermuth and H. U. Güdel, Chem. Phys. Lett. **281**, 81 (1997).
[12] M. P. Hehlen, N. J. Cockroft, T. R. Gosnell, A. J. Bruce, G. Nykolak, and J. Shmulovich, Opt. Lett. **22**, 772 (1997).
[13] P. Müller, M. Wermuth, and H. U. Güdel, Chem. Phys. Lett. **290**, 105 (1998).
[14] M. Wermuth, T. Riedener, and H. U. Güdel, Phys. Rev. B **57**, 4369 (1998).
[15] L. F. Johnson and H. J. Guggenheim, Appl. Phys. Lett. **20**, 474 (1972).
[16] A. J. Silversmith, W. Lenth, and R. M. Macfarlane, Appl. Phys. Lett. **51**, 1977 (1987).
[17] R. M. Macfarlane, F. Tong, A. J. Silversmith, and W. Lenth, Appl. Phys. Lett. **52**, 1300 (1988).
[18] T. J. Whitley, C. A. Millar, R. Wyatt, M. C. Brierley, and D. Szebesta, Electron. Lett. **27**, 1785 (1991).
[19] R. R. Stephens and R. A. McFarlane, Opt. Lett. **18**, 34 (1993).
[20] R. Brede, T. Danger, E. Heumann, G. Huber, and B. H. T. Chai, Appl. Phys. Lett. **63**, 729 (1993).
[21] R. J. Thrash and L. F. Johnson, J. Opt. Soc. Am. B **11**, 881 (1994).
[22] P. W. Binun, T. L. Boyd, M. A. Pessot, D. H. Tauimoto, and D. E. Hargis, Opt. Lett. **21**, 1915 (1996).
[23] T. Sandrock, H. Scheife, E. Heumann, and G. Huber, Opt. Lett. **22**, 808 (1997).
[24] R. Paschotta, P. R. Barber, A. C. Tropper, and D. C. Hanna, J. Opt. Soc. Am. B **14**, 1213 (1997).
[25] P. E.-A. Möbert, A. Diening, E. Heumann, G. Huber, and B. H. T. Chai, Laser Phys. **8**, 214 (1998).
[26] R. I. Laming, S. B. Poole, and E. J. Tarbox, Opt. Lett. **13**, 1084 (1988).
[27] L. B. Shaw, R. S. F. Chang, and N. Djeu, Phys. Rev. B **50**, 6609 (1994).
[28] S. A. Payne, G. D. Wilke, L. K. Smith, and W. F. Krupke, Opt. Commun. **111**, 263 (1994).
[29] Y. Guyot, H. Manaa, J. Y. Rivoire, R. Moncorgé, N. Garnier, E. Descroix, M. Bon, and P. Laporte, Phys. Rev. B **51**, 784 (1995).
[30] T. Chuang and H. R. Verdún, IEEE J. Quantum Electron. **32**, 79 (1996).
[31] S. Guy, C. L. Bonner, D. P. Shepherd, D. C. Hanna, A. C. Tropper, and B. Ferrand, IEEE J. Quantum Electron. **34**, 900 (1998).
[32] G. Rustad and K. Stenersen, IEEE J. Quantum Electron. **32**, 1645 (1996).
[33] M. Pollnau, IEEE J. Quantum Electron. **33**, 1982 (1997).
[34] M. Pollnau, P. J. Hardman, M. A. Kern, W. A. Clarkson, and D. C. Hanna, Phys. Rev. B **58**, 16 076 (1998).
[35] S. Singh and J. E. Geusic, Phys. Rev. Lett. **17**, 865 (1966).
[36] M. Pollnau, Th. Graf, J. E. Balmer, W. Lüthy, and H. P. Weber, Phys. Rev. A **49**, 3990 (1994).
[37] S. Guy, M. F. Joubert, B. Jacquier, and M. Bouazaoui, Phys. Rev. B **47**, 11 001 (1993).
[38] M. Pollnau, P. J. Hardman, W. A. Clarkson, and D. C. Hanna, Opt. Commun. **147**, 203 (1998).
[39] S. Guy, M. F. Joubert, and B. Jacquier, Phys. Rev. B **55**, 8240 (1997).
[40] D. L. Dexter, J. Chem. Phys. **21**, 836 (1953).
[41] S. O. Vasquez and C. D. Flint, Chem. Phys. Lett. **238**, 378 (1995).
[42] R. S. Quimby, W. J. Miniscalco, and B. Thompson, J. Appl. Phys. **76**, 4472 (1994).
[43] G. L. McPherson, J. A. Varga, and M. H. Nodine, Inorg. Chem. **18**, 2189 (1979).
[44] S. R. Lüthi, M. Pollnau, H. U. Güdel, and M. P. Hehlen, Phys. Rev. B **60**, 162 (1999).
[45] T. Riedener, P. Egger, J. Hulliger, and H. U. Güdel, Phys. Rev. B **56**, 1800 (1997).
[46] R. Burlot-Loison, M. Pollnau, K. Krämer, P. Egger, J. Hulliger, and H. U. Güdel (unpublished).
[47] D. R. Gamelin and H. U. Güdel, J. Am. Chem. Soc. **120**, 12 143 (1998).
[48] D. R. Gamelin and H. U. Güdel, Inorg. Chem. **38**, 5154 (1999).